PB90-265489

IC 9205

BUREAU OF MINES
INFORMATION CIRCULAR/1988

Emission Products From Combustion of Conveyor Belts

By Margaret R. Egan

UNITED STATES DEPARTMENT OF THE INTERIOR

50272-101

REPORT DOCUMENTATION PAGE	1. REPORT NO. BuMines IC 9205	2.	3. PB90-265489

4. Title and Subtitle Emission Products From Combustion of Conveyor Belts	5. Report Date 1988 6.
7. Author(s) Margaret R. Egan	8. Performing Organization Rept. No.
9. Performing Organization Name and Address U.S. Bureau of Mines Washington, DC 20241	10. Project/Task/Work Unit No. 11. Contract(C) or Grant(G) No. (C) (G)
12. Sponsoring Organization Name and Address Same	13. Type of Report & Period Covered 14.

15. Supplementary Notes

16. Abstract (Limit: 200 words)

A series of experiments were undertaken by the Bureau of Mines to determine the emission products of several types of conveyor belting and other combustible materials found in mines. These experiments were conducted under intermediate-scale, simulated mine conditions to determine smoke characteristics and gas concentrations. From these determinations, heat-release rates, particle sizes, obscuration rates, combustion yields, and production constants were calculated. Three types of belts were investigated: chloroprene, also known as neoprene (NP); polyvinyl chloride (PVC); and styrene-butadiene rubber (SBR). The belts were designated as ignitable or self-extinguishing depending on the length of the burning time and the subsequent combustion products. Under these experimental conditions, the SBR belts were the easiest to ignite. The PVC and NP belts tended to self-extinguish within a few minutes after ignition, but were still capable of maintaining a brief flaming period. These conveyor belt combustion results are compared with previous analyses of wood, transformer fluid, and coal fires. Together they form a data base by which findings from future experiments with other mine combustibles can be compared.

17. Document Analysis a. Descriptors

b. Identifiers/Open-Ended Terms

c. COSATI Field/Group

18. Availability Statement	19. Security Class (This Report)	21. No. of Pages
Unlimited release	Unclassified	19
	20. Security Class (This Page) Unclassified	22. Price

(See ANSI-Z39.18) See Instructions on Reverse

OPTIONAL FORM 272 (4-77)
(Formerly NTIS-35)
Department of Commerce

Information Circular 9205

Emission Products From Combustion of Conveyor Belts

By Margaret R. Egan

UNITED STATES DEPARTMENT OF THE INTERIOR
Donald Paul Hodel, Secretary

BUREAU OF MINES
T S Ary, Director

Library of Congress Cataloging in Publication Data:

Egan, Margaret R.

Emission products from combustion of conveyor belts.

(Bureau of Mines information circular; 9205)

Bibliography: p. 11

Supt. of Docs. no.: I 28.27:9205.

1. Conveyor belts—Fire - testing. 2. Combustion gases—Analysis. 3. Smoke—Analysis. I. Title. II. Series: Information circular (United States. Bureau of Mines); 9205.

TN295.U4 [TH9446.5.B44] 622 s [622'.8] 88-600216

CONTENTS

ILLUSTRATIONS

TABLES

UNIT OF MEASURE ABBREVIATIONS USED IN THIS REPORT

cfm	cubic foot per minute	kW	kilowatt
cm	centimeter	m	meter
g	gram	m^3/s	cubic meter per second
g/cm^3	gram per cubic centimeter	mg/m^3	milligram per cubic meter
g/g	gram per gram	min	minute
g/kJ	gram per kilojoule	μm	micrometer
$g/(m^3 \cdot ppm)$	gram per cubic meter times part per million	p/cm^3	particle per cubic centimeter
g/s	gram per second	p/g	particle per gram
kg	kilogram	p/kJ	particle per kilojoule
kJ/g	kilojoule per gram	ppm	part per million

EMISSION PRODUCTS FROM COMBUSTION OF CONVEYOR BELTS

By Margaret R. Egan[1]

ABSTRACT

A series of experiments were undertaken by the Bureau of Mines to determine the emission products of several types of conveyor belting and other combustible materials found in mines. These experiments were conducted under intermediate-scale, simulated mine conditions to determine smoke characteristics and gas concentrations. From these determinations, heat-release rates, particle sizes, obscuration rates, combustion yields, and production constants were calculated.

Three types of belts were investigated: chloroprene, also known as neoprene (NP); polyvinyl chloride (PVC); and styrene-butadiene rubber (SBR). The belts were designated as ignitable or self-extinguishing depending on the length of the burning time and the subsequent combustion products. Under these experimental conditions, the SBR belts were the easiest to ignite. The PVC and NP belts tended to self-extinguish within a few minutes after ignition, but were still capable of maintaining a brief flaming period.

These conveyor belt combustion results are compared with previous analyses of wood, transformer fluid, and coal fires. Together they form a data base by which findings from future experiments with other mine combustibles can be compared.

[1]Chemist, Pittsburgh Research Center, Bureau of Mines, Pittsburgh, PA.

INTRODUCTION

The Bureau of Mines conducts research to improve health and safety conditions in mines. Fires are particularly dangerous in underground mines because of the added threat of smoke and toxic gases being carried throughout the mine by its ventilation system. Therefore, the Bureau has analyzed the combustion emissions of materials found in mines.

The objectives of this study were to measure the gas production and smoke characteristics of burning conveyor belts, and to compare these results with those of other combustible materials previously studied. Once the gas concentrations and smoke characteristics of combustible materials are determined, more efficient detection, suppression, and rescue equipment can be designed.

This report supplements previous Bureau studies (*1-3*)[2] of other combustible materials burned in a test apparatus designed to simulate a mine environment. This study focused on conveyor belting because of the significant quantities used and their possible location on the air-intake side of the ventilating system. Determining the fire resistance of conveyor belts was presented in a previous Bureau report (*4*), and was not part of this study.

EXPERIMENTAL EQUIPMENT

INTERMEDIATE-SCALE FIRE TUNNEL

The conveyor belt fires were conducted in the Bureau's intermediate-scale fire tunnel. This tunnel has been shown (*5*) to successfully predict full-scale fire conditions. A schematic of the tunnel with its data-acquisition system is shown in figure 1.

The tunnel is 0.8 m wide by 0.8 m high by 10 m long and is divided into several sections. The first horizontal section is cone-shaped and 1.5 m long. It is hinged and can be lifted to allow entrance into the tunnel for the placement of the belting. It begins with a cylindrical duct that is 0.25 m long by 0.3 m in diameter and gradually enlarges until it matches the tunnel dimensions. Next is the fire zone where the gas burner and the conveyor belt platform are located. The fire zone and the remaining horizontal section are lined with firebrick and contain the thermocouples, flow probes, and sampling ports. The diffusing grid begins the vertical section of the tunnel, which contains an adjustable orifice plate. The final section is horizontal and ends at an exterior exhaust fan.

DATA LOGGING

The tunnel was equipped with a 48-channel data collection system. A program was designed to scan, record, and calculate the data from all channels including a number of cross-channel calculations. These calculations and the raw voltage readings are stored, displayed, and updated every minute throughout the experiment.

INSTRUMENTATION

All instruments were periodically cleaned and calibrated according to manufacturers' instructions for the quantity of smoke and the amount of use each had received.

THERMOCOUPLES

Thermocouple arrays were located 1.57, 2.36, 3.15, 4.72, 6.30, and 7.87 m from the gas burner. Additional thermocouples were located within the air-intake cone and near the exhaust fan. A total of 28 thermocouples were used to measure the temperature distributions resulting from the fires. Their locations are also shown in figure 1.

FLOW PROBES AND PRESSURE TRANSDUCERS

A bidirectional flow probe (*6*) in conjunction with a pressure transducer was used to determine velocity. The airflow was produced by the exhaust fan and was detected by the flow probe and converted to a linear electrical signal by the pressure transducer. This signal was then scanned, stored, and converted to cubic meter per second by the data collection system. The locations of all of the flow probes are shown in figure 1. The flow probe centered in the air-intake cylinder was used to obtain the velocity measurements.

The stated error of the flow probe is ±7%. The pressure transducer introduces another possible error of ±5.3%. Assuming the errors to be independently distributed, the compound error was estimated to be ±8.8%. Averaging over 10 data points improves the precision by the square root of 10, resulting in a total estimated error of ±2.8%.

Before each experiment, velocity readings were also made with a vane-type anemometer to insure that the air-intake velocity was approximately the same for all tests.

GAS MONITORS

The CO analyzer used measures accurately within 1% of full range or ±5 ppm. The CO_2 analyzer measures accurately within 1% of full range or ±250 ppm. These

[2]Italic numbers in parentheses refer to items in the list of references preceding the appendix at the end of this report.

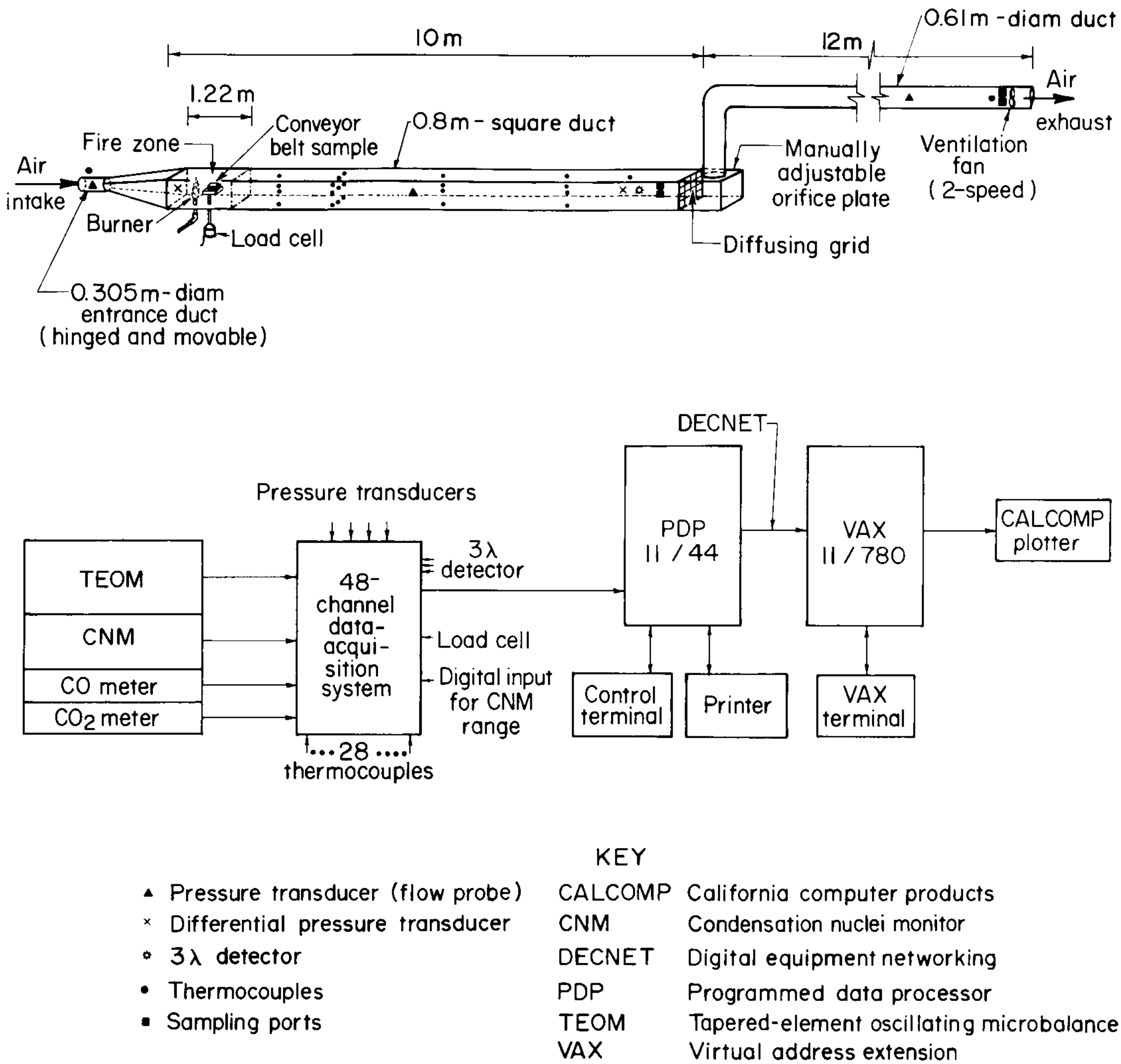

Figure 1.—Schematic of intermediate-scale tunnel (top) and data-acquisition system (bottom).

analyzers were calibrated at the beginning of each experiment. In addition, the concentrations of the span gases were independently analyzed at the beginning of each series of experiments.

SMOKE MONITORS

The particle number concentration (N_o) was obtained with a condensation nuclei monitor (CNM), manufactured by Environment One Corp.[3] of Schenectady, NY. This monitor uses a cloud chamber to measure the concentration of submicrometer airborne particles (p). The particulate cloud attenuates a light beam which ultimately produces a measurable electrical signal. The accuracy is stated as ±20% of a point above 30% of scale within the linear range from 3,000 to 300,000 p/cm^3. Therefore, in these experiments, the calculated error could have been as great as ±18,000 p/cm^3.

To reduce the particulate count to within the range of the CNM, a 10% dilution of the smoke was necessary. Two flow meters, with a stated accuracy of ±2%, were used. One meter was used to measure the flow of the sample, and the other to measure filtered room air. Compounding these errors makes the CNM the least accurate of all the instruments at ±21%. The particle mass concentration (M_o) was obtained by a tapered-element oscillating microbalance (TEOM) developed by Rupprecht & Patashnick Co., Inc. (*7*) of Voorheesville, NY. It measures the mass directly by depositing the particles on a filter attached to an oscillating tapered element. The oscillating frequency of the tapered element decreases as the deposited mass increases. The apparatus is capable of measuring the particulate concentration with a better than 5% accuracy at the level used. According to the manufacturer, the filter collects at least 50% of all particles with a volume mean diameter of 0.05 µm, with increasing collection efficiency as the diameter increases. Actual data obtained by the Bureau using particles of volume mean diameter equal to 0.048 µm indicated a collection efficiency closer to 90%.

Since the diameter of average mass was calculated from the mass and number concentrations, its accuracy was dependent upon the precision of the TEOM and CNM. Considering the error band of the mass and number concentrations from the conveyor belt experiments, the diameter of average mass could vary by 10%.

A three-wavelength-light transmission technique (*8*) developed by the Bureau was also used to measure particle size and smoke obscuration. White light was transmitted through a smoke cloud to the detector. The beam was split into three parts, and each passed through an interference filter centered at wavelengths of either 0.45, 0.63, or 1.00 µm. Each photodiode output was amplified and the voltage was recorded.

WEIGHT-LOSS MONITOR

The weight-loss data were obtained by a strain-gauge conditioner in conjunction with a load cell that has a range up to 22.68 kg. Their combined accuracy is stated as 0.05% of full scale or ±11.3 g.

TYPICAL TEST PROCEDURE

The conveyor belt was located 43 cm from the ceiling of the tunnel. A 23- by 46-cm section was attached to a support that was six-legged and approximately 15 cm high. The support sat on a platform attached to a shaft extending through a hole in the tunnel floor. The shaft rested on a load cell so that continuous weight loss could be recorded.

Prior to each experiment, background readings were obtained after the conveyor belting was positioned and the exhaust fan was started. All instruments were continuously scanned and recorded throughout the experiment.

The belts were heated with a natural gas burner located immediately upstream of the belt. The burner flow rate was maintained at 7 cfm until the belt was ignited. The flame was perpendicular to the front end of the belt and was pulled over its surface by the ventilation. Once ignition occurred, the burner was turned off. The flames either spread along the top surface of the belt or extinguished within a few minutes.

CALCULATIONS

It is necessary to measure certain parameters in order to compare the active-burning combustion products and ultimately the hazards of various fuels. Among these measurements are gas concentrations, smoke particle mass and number concentrations, ventilation rate, and mass-loss rate. Other combustion properties can be calculated once these values are known.

[3]Reference to specific products does not imply endorsement by the Bureau of Mines.

PRODUCT GENERATION RATES

In a ventilated system, the generation rates ($\dot{G}_X$) of CO_2 and CO are related to the bulk average concentration increases above ambient air, ΔCO_2 and ΔCO respectively, by the expressions

$$\dot{G}_{CO_2} = M_{CO_2} \times V_oA_o \times \Delta CO_2 \quad (1)$$

and

$$\dot{G}_{CO} = M_{CO} \times V_oA_o \times \Delta CO, \quad (2)$$

where M_{CO_2} = 1.97×10^{-3} g/(m^3•ppm),

M_{CO} = 1.25×10^{-3} g/(m^3•ppm),

and V_oA_o = incoming airflow, m^3/s.

COMBUSTION YIELDS

Once the generation rates are known and the mass-loss rate of the fuel ($\dot{M}_f$) is calculated using the load-cell assembly, the yield of the combustion product (Y_x) can be calculated by the expression

$$Y_X = \dot{G}_X/\dot{M}_f. \quad (3)$$

The yields for M_o and N_o are calculated in a similar manner by the expression

$$Y_X = \Delta X\,(C_X)(V_oA_o)/\dot{M}_f, \quad (4)$$

where C_X = appropriate units conversion factor: 1.00×10^{-3} when M_o is in milligram per cubic meter or 1.00×10^{6} when N_o is in particle per cubic centimeter;

and ΔX = smoke concentration increase above ambient (when M_o is measured in milligram per cubic meter and N_o is measured in particle per cubic centimeter.

HEAT-RELEASE RATES

It has been shown (*9*) that the actual heat-release rate realized during a fire can be calculated from the expression

$$\dot{Q}_A = \left(\frac{H_C}{K_{CO_2}}\right)\dot{G}_{CO_2} + \left[\frac{H_C - H_{CO}\,(K_{CO})}{K_{CO}}\right]\dot{G}_{CO}, \quad (5)$$

where $\dot{Q}_A$ = actual heat release, kW,

H_C = net heat of complete combustion of the conveyor belting, kJ/g,

H_{CO} = heat of combustion of CO (10.1 kJ/g),

K_{CO_2} = theoretical yield of CO_2, g/g,

and K_{CO} = theoretical yield of CO, g/g.

The H_C and K_x values vary with the composition of the belt. The values, listed in table 1, were derived from the ultimate chemical analyses and the caloric values determined by an independent testing laboratory. The actual heat-release rates could be calculated by substituting the experimental values for V_oA_o, ΔCO_2, and ΔCO and those from table 1 in equations 1, 2, and 5. The actual heat of combustion (H_A) is lower than the net heat of combustion (H_C) since a typical fire rarely attains a state of complete combustion. By measuring both $\dot{Q}_A$ and $\dot{M}_f$, H_A can be calculated from the expression

$$H_A = \dot{Q}_A/\dot{M}_f. \quad (6)$$

This was only possible for the more easily ignited belts because the mass loss for the other belts was too small to be accurately determined.

PRODUCTION CONSTANTS

In an actual mine fire, it is difficult, if not impossible, to calculate the actual heat of combustion. Moreover, since determining the yield of a combustion product depends upon this information, significant errors can result in predicting the resultant concentration increases. For fires,

TABLE 1. - Heat release equation variables for conveyor belts

Sample	H_C, kJ/g	K_{CO}, g/g	K_{CO_2}, g/g
IGNITABLE			
R1	36.84	1.83	2.88
R2	29.07	1.49	2.35
R3	29.20	1.52	2.39
R5	28.88	1.50	2.35
SELF-EXTINGUISHING			
R4	18.65	1.06	1.66
R8	27.89	1.41	2.22
P1	23.43	1.21	1.90
P2	24.11	1.21	1.90
P3	24.33	1.15	1.80
P5	27.21	1.26	1.97

the hazards tend to increase with the actual heat-release rate. For this reason, production constants, or beta values (β_X), can be calculated for a given product by the expression

$$\beta_X = \dot{G}_X/\dot{Q}_A. \tag{7}$$

Using the rate of formation of gas or smoke as a function of the fire size is also beneficial in comparing the combustion hazards of different materials.

SMOKE PARTICLE DIAMETERS

Measurements of both number and mass concentrations of the smoke provide important information relative to the yields (equation 4) and production constants (equation 6). They can also be used to calculate the average size of the smoke particles, using the expression

$$\frac{\pi d_m^3}{6} (\rho_p)(N_o) = 1 \times 10^3 M_o, \tag{8}$$

where ρ_p = individual particle density, g/cm^3,

d_m = diameter of average mass, μm,

and 1×10^3 = the appropriate units conversion factor.

Assuming the approximate density of the base material to be 1.4 g/cm^3, the diameter of average mass can be calculated from

$$d_m = 11.09 \left[\frac{M_o}{N_o}\right]^{1/3} \tag{9}$$

when the particle diameter is expressed in micrometers.

Using the three-wavelength smoke detector, the transmittance (T) of the light through the smoke can be calculated for each wavelength. The extinction-coefficient ratio can be calculated for each pair of wavelengths (λ) from the following log-transmission ratios:

$$\frac{\ln T(\lambda 1.00)}{\ln T(\lambda 0.63)}, \quad \frac{\ln T(\lambda 1.00)}{\ln T(\lambda 0.45)}, \text{ or } \frac{\ln T(\lambda 0.63)}{\ln T(\lambda 0.45)}.$$

Using these extinction coefficients and the curve in figure 11 of reference 8, the surface mean particle size (d_{32}) can be determined. (Calculation of the extinction-coefficient curves assumes spherical particles with an estimated refractive index.)

The smoke obscuration is the percentage of light absorbed by the smoke or 100% of the light minus the percent transmission (T). It is calculated using the following equation:

$$\text{Obscuration} = 100(1 - T) \tag{10}$$

The obscuration percentages presented in this report are an average of those calculated from the two visible wavelengths, 0.45 μm and 0.63 μm.

CONVEYOR BELT COMBUSTION RESULTS AND DISCUSSION

The compositions of the 10 different belt types tested are listed in table 2. Because of their unique composition and construction, each belt had distinctive burning times and combustion products. Table 2 also lists the designations and burning times for each belt tested. The burning times were calculated from the time the burner was turned off until flames were no longer visible. The intensities of the belt fires were not considered; therefore, the burning times include rapid burning as well as the flickering flames of the quickly extinguished belts.

All belt tests were duplicated or triplicated depending on the amount of sample available. The values for the ignitable belts listed in the following tables are averaged during the rapidly burning stage without the burner operating. Since the self-extinguishing belts did not burn readily, their averages may also include some residual effects of the burner.

Figure 2 shows a typical ignitable belt (R5). In this experiment, the gas burner was turned off at 9 min. Its effects can be seen until the 12th minute. This belt burned for approximately 28 min before it self-extinguished. Figure 3 shows the extent of the combustion as well as the charring for R5.

TABLE 2. - Conveyor belts analyzed

Sample	Material	Burning time, min
	IGNITABLE	
R1	Styrene Butadiene Rubber (SBR)	28.5
R2	do	25.5
R3	do	51.5
R5	do	28.3
	SELF-EXTINGUISHING	
R4	Neoprene (NP)	15.0
R8	do	17.5
P1	Polyvinly Chloride (PVC)	6.0
P2	do	14.5
P3	do	3.0
P5	do	7.5

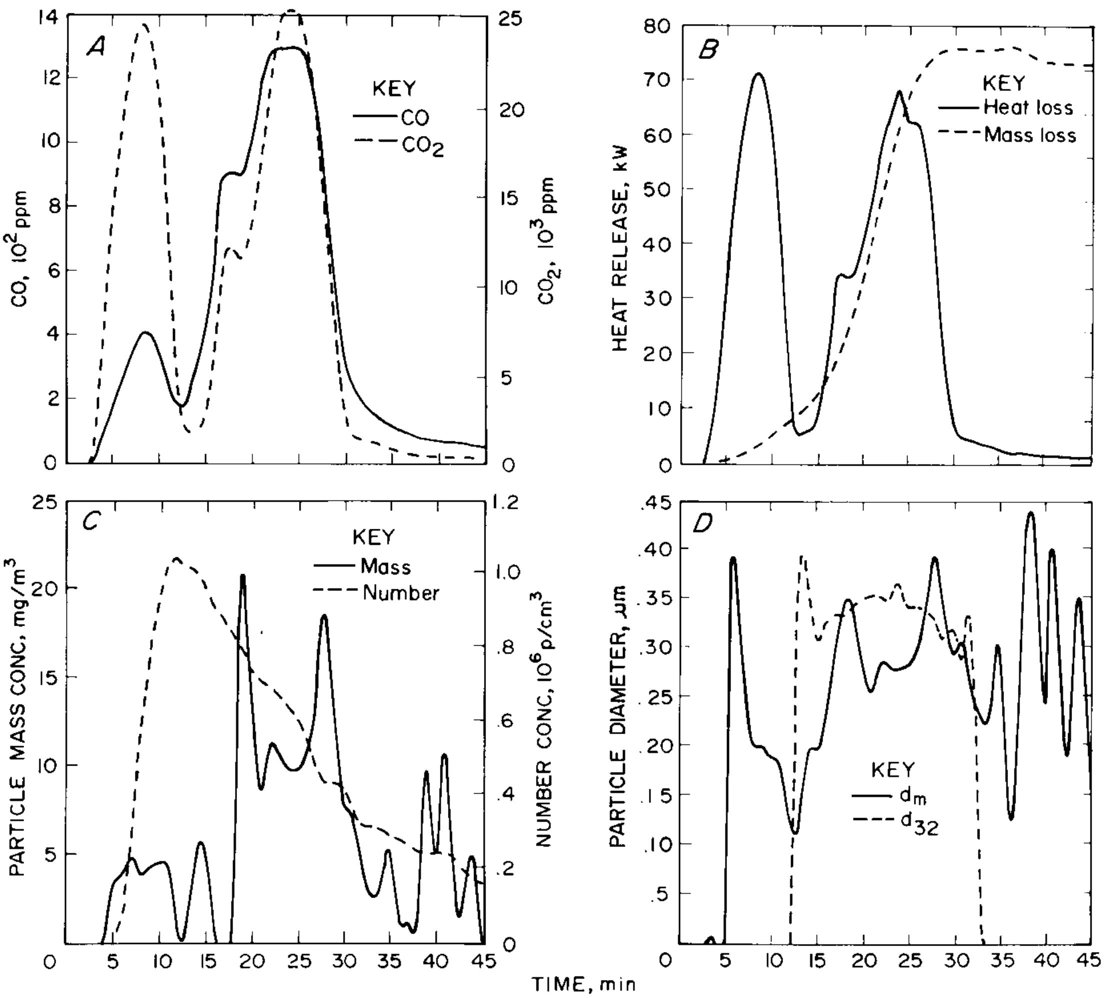

Figure 2.—Results of typical ignitable conveyor belt combustion experiment. *A*, CO and CO_2 concentrations; *B*, heat-release and mass-loss rates; *C*, particle mass and number concentrations; and *D*, diameter of average mass (d_m) and mean particle diameter (d_{32}).

GAS CONCENTRATIONS AND HEAT PRODUCTION

Figure 2*A* illustrates CO and CO_2 production. The initial spike is caused by the gas burner, which was turned off once the belt ignited. Several minutes were required for the contaminating gases to be dispersed. The belt was rapidly burning from the 15th to the 30th minute.

Table 3 lists the CO and CO_2 concentrations and generation rates and the corresponding heat-release rates. All the values for the ignitable belts are higher than those for the self-extinguishing belts. The CO and CO_2 concentrations listed for the self-extinguishing belts, although much lower than those from the ignitable belts, may still include residual gas from the burner.

Figure 2*B* correlates the heat-release rate with the mass loss. As expected, the most heat was released during the

TABLE 3. - Gas concentrations, generation rates, and heat-release rates for conveyor belts

Sample	CO, ppm	CO_2, ppm	G_{CO}, 10^{-2} g/s	G_{CO_2}, g/s	Q_A, kW
IGNITABLE					
R1	1,044	16,830	14.7	3.72	49.08
R2	778	14,102	10.7	3.06	38.90
R3	753	10,213	9.7	2.07	26.24
R5	1,032	13,940	14.6	3.09	39.31
SELF-EXTINGUISHING					
R4	75	510	0.9	0.14	1.79
R8	78	432	1.3	.11	1.51
P1	62	632	.9	.14	1.79
P2	44	637	.6	.14	1.77
P3	213	1,405	2.9	.30	4.37
P5	172	1,263	2.4	.28	4.14

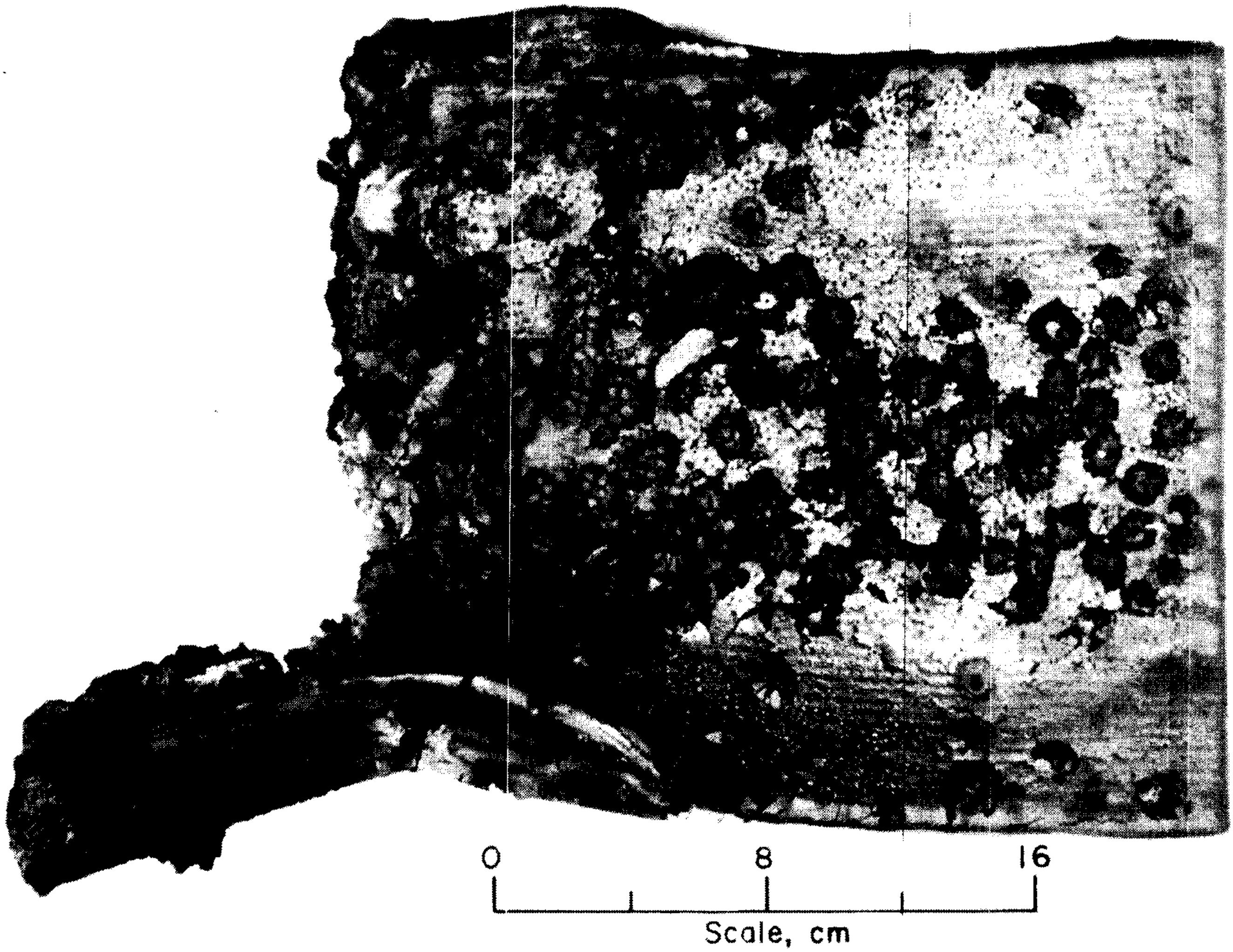

Figure 3.—Extent of the combustion and charring for R5.

greatest mass loss. Most ignitable belts lost about 1 g/s during the rapidly burning stage. The mass-loss rates of the self-extinguishing belts were too small to be determined.

SMOKE CHARACTERISTICS

Figure 2*C* shows the typical M_0 and N_0. The M_0 rose slightly when the gas burner was ignited. It fluctuated after the burner was turned off, but shows a sustained increase during the rapidly burning stage. As the flames died, the mass concentration decreased, but increased again as the belt smoldered.

The N_0 rose steadily in response to the gas burner and declined after burner extinguishment throughout the rapidly burning and smoldering stages. Most belts, as this one, did not produce a distinct number concentration peak during the rapidly burning stage.

TABLE 4. - Smoke characteristics for conveyor belts

Sample	N_0, 10^4 p/cm³	M_0, mg/m³	d_m, µm
IGNITABLE			
R1	16.65	91.95	0.92
R2	17.59	23.50	.56
R3	20.80	45.35	.49
R5	17.21	14.05	.49
SELF-EXTINGUISHING			
R4	19.12	5.10	0.26
R8	6.02	4.05	.47
P1	29.53	1.80	.37
P2	28.02	1.70	.33
P3	ND	.60	ND
P5	35.31	2.05	.19

ND Not determined.

TABLE 5. - Mean particle sizes and smoke obscuration for conveyor belts

Test	lnT(λ1.00)/lnT(λ0.63) Average, µm	lnT(λ1.00)/lnT(λ0.63) Range, µm	lnT(λ1.00)/lnT(λ0.45) Average, µm	lnT(λ1.00)/lnT(λ0.45) Range, µm	lnT(λ0.63)/lnT(λ0.45) Average, µm	lnT(λ0.63)/lnT(λ0.45) Range, µm	Average d_{32}, µm	Obscuration, %
IGNITABLE								
R1	0.39	0.35 - 0.41	0.32	0.22 - 0.38	0.26	0.15 - 0.35	0.33	85
R2	.38	.35 - .39	.26	.17 - .30	.19	.17 - .24	.29	90
R3	.36	.34 - .40	.35	.22 - .50	.41	.21 - .66	.36	75
R5	.39	.34 - .40	.35	.34 - .37	.33	.30 - .36	.35	97
SELF-EXTINGUISHING								
R4	0.35	0.33 - 0.37	0.23	0.23 - 0.24	ND	NAp	0.29	22
R8	ND	NAp	ND	NAp	ND	NAp	ND	ND
P1	ND	NAp	ND	NAp	ND	NAp	ND	5
P2	ND	NAp	ND	NAp	ND	NAp	ND	8
P3	ND	NAp	ND	NAp	ND	NAp	ND	12
P5	.35	.33 - .36	.28	.26 - .31	0.22	0.17 - 0.27	0.29	46

ND Not determined.
NAp Not applicable.

The smoke characteristics data are presented in tables 4 and 5. A high mass concentration for belt R1 was reproduced in duplicate tests and so was considered valid. Using these data, a large calculated d_m results.

The average particle size, d_{32}, calculated from the three-wavelength transmission technique shows less variation than d_m. The smoke obscuration must be at least 15% before d_{32} can be calculated. Only two self-extinguishing belts, R4 and P5, produced enough smoke to secure this data. Since all the diameters are in the same range, there may not be a significant difference when comparing either the method of calculation or the flammability of the belts. Figure *2D* shows the particle diameters as calculated by both methods. The d_{32} data were only calculated from the 12th to the 33rd minute because the smoke obscuration was above 15% in that period. The best agreement is seen during the rapidly burning stage.

COMBUSTION YIELDS

The mass-loss rates of the self-extinguishing belts were too low to accurately calculate their combustion yields. Table 6 contains the average yields for the ignitable belts. The high mass concentration for R1 is once again evident. R3 had the highest mass-loss rate, 1.3 g/s, which contributes to the relatively low yields.

PRODUCTION CONSTANTS

Table 7 lists the production constants (or beta values). They are scaled according to their fire size. The production constants for CO and CO_2 remain fairly constant for all tests. However, the production constant for the number concentration changes considerably because the fire size of the flammable belts is much larger than for the self-extinguishing belts while the number concentration remains about the same. The production constants of all the belts for mass concentration also remain fairly constant because the mass concentrations increased proportionally with the fire size.

SMOLDERING STAGE DATA

For most belts, the collection of data continued after the visible flames had subsided. Table 8 shows the results of the smoldering stage. The smoldering time states the length of the data collection period, and does not reflect the complete smoldering period.

These data were included to provide a comparison between the smoke characteristics of flaming and smoldering belts. In most belt tests, the d_m was smaller during the smoldering than the flaming stage, but the opposite was generally true for d_{32}. As M_o and N_o decreased, the calculated particle size decreased. However, as the obscuration decreased, the particles were slightly larger. The closest agreement with the flaming particle size is found when calculating d_{32}.

TABLE 6. - Combustion yields for ignitable conveyor belts

Test	Y_{CO}, 10^{-2} g/g	Y_{CO_2}, g/g	Y_{N_o}, 10^{10} p/g	Y_{M_o}, 10^{-3} g/g
R1	17.2	4.4	2.2	12.2
R2	13.3	3.7	2.3	3.2
R3	8.4	1.9	1.5	4.8
R5	16.3	3.4	2.2	1.7

TABLE 7. - Steady-state production constants for conveyor belts

Sample	β_{CO}, 10^{-3} g/kJ	β_{CO_2}, 10^{-2} g/kJ	β_{N_o}, 10^{8} p/kJ	β_{M_o}, 10^{-4} g/kJ
IGNITABLE				
R1	2.99	7.58	3.81	2.11
R2	2.76	7.87	4.99	.67
R3	3.71	7.91	8.19	1.79
R5	3.71	7.86	4.94	.40
SELF-EXTINGUISHING				
R4	7.84	8.38	159.73	4.26
R8	8.61	7.28	51.49	3.46
P1	4.83	7.75	184.06	1.12
P2	3.45	7.85	175.55	1.07
P3	6.61	6.86	ND	.15
P5	5.80	6.76	96.12	.56

ND Not determined.

TABLE 8. - Smoldering data for conveyor belts

Sample	Smoldering time, min	N_o, 10^4 p/cm^3	M_o, mg/m^3	d_m, µm	d_{32}, µm	Obscuration, %
IGNITABLE						
R1	2.0	2.43	1.24	0.47	0.39	16
R2	7.5	2.94	1.33	.45	.30	28
R3[1]	ND	ND	ND	ND	ND	ND
R5	20.0	18.58	1.58	.24	.29	48
SELF-EXTINGUISHING						
R4	12.0	40.03	6.85	0.32	0.30	19
R8	10.0	3.82	1.36	.34	ND	ND
P1	3.3	29.01	8.48	.28	ND	ND
P2	3.5	9.69	1.58	.27	ND	ND
P3	1.5	29.50	1.74	.23	ND	ND
P5	3.0	29.67	2.22	.19	.31	35

ND Not determined.
[1]Smoldering stage data were not collected.

COMPARISON OF MATERIALS TESTED

Smoke detection has been raised to a high level of sophistication in order to detect fires in their earliest stages, and to discriminate between actual fires and emissions that are not fire related. In this effort, the smoke characteristics of various materials have been analyzed. Earlier studies of wood, coal, and transformer fluid were conducted in the same intermediate-scale fire tunnel using the same instrumentation and calibration techniques. The different combustion kinetics of each material tested necessitated a modification of some of the experimental conditions such as ventilation rates and ignition sources (table 9).

The gas, heat, and smoke concentrations for the four materials studied are found in table 10. The highest gas concentration was produced by the ignitable conveyor belts, but the highest heat release was produced by wood fires. The configuration of the wooden sticks may have improved the air circulation, which could have supported more complete combustion than was achieved using the other fuels. For better comparison, the emission products of the other fuels were adjusted, based on their production constants, to the level of the wood fires.

Table 11 gives normalized values of the data in table 10. At this projected fire intensity, burning coal generally produced the most hazardous emissions. However, the true assessment of the hazards of burning materials cannot be determined solely on their emission products. Their physical characteristics and composition must also be considered. For example, the extremely rapid growth rate and thick smoke of liquid fuels fires such as transformer fluid increases their potential danger. By comparison, the combustion of the synthetic components of PVC conveyor belts may produce high levels of toxic gas and smoke, but because they self-extinguish their relative dangers are reduced. An estimation of the potential danger of burning materials must not only include their smoke characteristics, but also the toxic environment that their combined emissions may create.

Most smoke detectors sense an increase in the number and size of the particulate matter. In these experiments, burning conveyor belts produced a thick smoke obscuring on an average 87% of the light. The particle size of the flammable belts tended to be larger than the other materials tested. The particle size and obscuration values are listed in table 12. The higher the smoke concentration the more dangerous are the effects from a fire, but the more detectable it becomes.

The production constants (table 13) use the heat release to compare the rate of formation of gas or smoke. Burning coal generated the highest number of smoke particles, and transformer fluid generated the largest mass concentration. Since ignitable belts burn with such a high heat release, the production constants remain relatively low especially for M_o and N_o.

All combustion generates some amount of smoke. The characteristics of this smoke depend not only upon the composition of the material, but the conditions in which it is burning. In an attempt to standardize these experiments, conditions may have been used that were not optimum for all materials. These limitations must be considered when comparing the gas concentrations and smoke characteristics given in this report.

TABLE 9. - Ignition source and ventilation rates

Material	Ignition source	V_oA_o, m^3/s
Wood	Natural gas burner	1.0
Coal	Electric strip heaters	.24
Transformer fluid	Natural gas burner	.47
Conveyor belts	... do	.11

TABLE 10. - Gas, heat, and smoke concentrations

Material	CO, ppm	CO_2, ppm	Q_A, kW	N_o, 10^6 p/cm^3	M_o, mg/m^3
Wood	145	6,759	110.2	6.0	49.1
Coal	89	1,095	5.9	1.5	11.4
Transformer fluid	113	1,769	21.1	1.1	35.3
Ignitable belts	902	13,771	38.4	.2	43.7
Self-extinguishing belts	107	813	2.6	.2	2.6

TABLE 11. - Normalized gas and smoke concentrations

Material	CO, ppm	CO_2, ppm	N_o, 10^6 p/cm^3	M_o, mg/m^3
Wood	145	6,759	6.0	49.1
Coal	441	5,762	7.12	50.6
Transformer fluid	284	4,992	2.79	85.2
Ignitable belts	294	5,017	.01	13.5
Self-extinguishing belts	528	4,480	1.08	12.1

TABLE 12. - Particle size and smoke obscuration

Material	d_m, µm	d_{32}, µm	Obscuration, %
Wood	0.22	ND	9
Coal	.21	0.23	20
Transformer fluid	.39	.39	46
Ignitable belts	.62	.33	87
Self-extinguishing belts	.32	.29	18

ND Not determined.

TABLE 13. - Production constants

Material	β_{CO}, 10^{-3} g/kJ	β_{CO_2}, 10^{-2} g/kJ	β_{N_o}, 10^{10} p/kJ	β_{M_o}, 10^{-4} g/kJ
Wood	1.6	10.4	5.79	4.9
Coal	4.8	8.9	6.83	4.7
Transformer fluid	3.1	7.7	2.48	7.8
Ignitable belts	3.2	7.8	.05	1.2
Self-extinguishing belts	5.8	6.9	1.04	1.1

CONSIDERATIONS

Burning materials generate unique and dangerous combustion products. In a mine fire, these emissions combine to produce a wide variety of smoke particles and volatile gases that are transported by the ventilating system. If the individual smoke characteristics and combustion products were known, more discriminating or sensitive smoke detectors could be developed. For example, the presence of exhaust emissions could be distinguished from the products of a real fire, eliminating many false alarms. Thus, the remaining alarms would elicit an immediate response instead of a delay caused by the need to confirm the alarm. This would further the efforts of the Bureau to improve health and safety conditions in mines. With this goal in mind, these experiments were conducted to compare the potential detectability of the smoke generated by combustible materials found in underground mines.

REFERENCES

1. Egan, M. R., and C. D. Litton. Wood Crib Fires in a Ventilated Tunnel. BuMines RI 9045, 1986, 18 pp.
2. Egan, M. R. Transformer Fluid Fires in a Ventilated Tunnel. BuMines IC 9117, 1986, 13 pp.
3. ___. Coal Combustion in a Ventilated Tunnel. BuMines IC 9169, 1987, 13 pp.
4. Sapko, M. J., K. E. Mura, A. L. Furno, and J. M. Kuchta. Fire Resistance Test Methods for Conveyor Belts. BuMines RI 8521, 1981, 27 pp.
5. Lee, C. K., R. F. Chaiken, J. M. Singer, and M. E. Harris. Behavior of Wood Fires in Model Tunnels Under Forced Ventilation Flow. BuMines RI 8450, 1980, 58 pp.
6. McCaffrey, B. J., and G. Heskestad. A Robust Bidirectional Low-Velocity Probe for Flame and Fire Application. Combust. and Flame, v. 26, No. 1, 1976, pp. 125-127.
7. Patashnick, H., and G. Rupprecht. Microweighing Goes On-Line in Real Time. Res. and Dev., v. 28, No. 6, 1986, pp. 74-78.
8. Cashdollar, K. L., C. K. Lee, and J. M. Singer. Three-Wavelength Light Transmission Technique To Measure Smoke Particle Size and Concentration. Appl. Optics, v. 18, No. 11, 1979, pp. 1763-1769.
9. Tewarson, A. Heat Release Rate in Fires. Fire and Mater., v. 4, No. 4, 1980, pp. 185-191.

APPENDIX.–SYMBOLS USED IN THIS REPORT

C_X	conversion factor of given combustion product
d_m	diameter of a particle of average mass, µm
d_{32}	mean particle size, µm
$\dot{G}_X$	generation rate of a given combustion product, g/s
H_A	actual heat of combustion, kJ/g
H_C	net heat of combustion of material, kJ/g
H_{CO}	heat of combustion of CO, kJ/g
K_X	theoretical yield of a given gas, g/g
ln	logarithm, natural
$\dot{M}_f$	fuel mass loss rate, g/s
M_o	particle mass concentration, mg/cm^3
M_X	density of a given gas, $g/(m^3 \bullet ppm)$
N_o	particle number concentration, p/cm^3
p	particle
$\dot{Q}_A$	actual heat-release rate, kW
T	transmission of light
V_oA_o	ventilation rate, m^3/s
Y_X	yield of a given combustion product, g/g or p/g
β_X	production constant of a given combustion product, g/kJ or p/kJ
ΔX	measured change in a given quantity, ppm
λ	wavelength, µm
ρ_p	individual particle density, g/cm^3

* U.S. GOVERNMENT PRINTING OFFICE: 611-012/00,022

INT.-BU.OF MINES,PGH.,PA.28805